Simulation Methodologies for Acoustic Noise Induced by Multilayer Ceramic Capacitors of Power Distribution Network in Mobile Systems

Yin Sun, *Student Member, IEEE*, Songping Wu, *Senior Member, IEEE*, Jianmin Zhang, *Senior Member, IEEE*, Chulsoon Hwang, *Senior Member, IEEE*, and Zhiping Yang, *Senior Member, IEEE*

***Abstract*—In this article, multilayer ceramic capacitors (MLCCs) induced acoustic noise is studied through simulation investigation of the vibration behavior of the printed circuit board (PCB). The board vibration theory is briefly summarized to understand the key parameters influencing intrinsic board vibration properties. The identified key parameters are the thickness, mass density, and Young's modulus of each board layer. To accommodate the parameter variations in real board fabrication process, a statistical simulation model for PCB vibration modal response is proposed. The simulation results have shown good correlation with the measurement. The sensitivity analysis of board vibration properties to the identified parameters of each layer has also been conducted through simulation. Based on the derived intrinsic board vibration properties, the PCB vibration behavior with capacitor as forced excitation is further analyzed through modal superposition. The simulated results also exhibit good correlation with measurement. With the proposed simulation methods, engineers can evaluate the board vibration behavior at early design stage and some design guidelines for placing MLCCs can be derived to reduce acoustic noise.**

***Index Terms*—Acoustic noise, harmonic analysis, mass density, modal analysis, thickness, vibration, Young's modulus.**

I. Introduction

MULTILAYER ceramic capacitors (MLCCs) has been widely applied as decoupling capacitors for the power distribution network (PDN) in modern mobile systems. The electrical performance of PDN has been investigated extensively [1]–[3]. The influence of MLCC package size, power, and ground via pinout and voltage derating are commonly evaluated as the criteria for MLCC selection and placement. The improvement of the electrical characteristics of PDN is important as the performance of the integrated circuits in the mobile system relies on it significantly [4].

Manuscript received December 15, 2019; revised April 20, 2020 and July 13, 2020; accepted August 16, 2020. This work was supported in part by the National Science Foundation under Grant IIP-1140110 and in part by the Google Inc. *(Corresponding author: Yin Sun.)*

Yin Sun and Chulsoon Hwang are with the EMC Laboratory, Missouri University of Science and Technology, Rolla, MO 65401 USA (e-mail: ysc26@mst.edu; hwangc@mst.edu).

Songping Wu, Jianmin Zhang, and Zhiping Yang are with the Google Inc., Mountain View, CA 94043 USA (e-mail: songpingwu@google.com; jianmin@google.com; zhipingyang@google.com).

Color versions of one or more of the figures in this article are available online at https://ieeexplore.ieee.org.

Digital Object Identifier 10.1109/TEMC.2020.3019438

PDN with improved electrical performance is one of the crucial foundations for better user experience. Recently, another aspect for MLCC and PDN consideration has starting to draw attention [5]. The MLCC induced high pitch acoustic noise in mobile systems could be a serious concern for user experience and should be evaluated during the PCB design stage. The dielectric material is $BaTiO_3$ which allows the realization of capacitor with large capacitance value in a compact package size. An additional effect this material brings is the piezoelectric property. With the ac electrical noise presented on PDN, the MLCCs start to contract and expand following the pace of the electrical noise [6]. The MLCCs vibration can then be transferred to PCB. If the electrical noise is in the range of audible frequency (20–20 000 Hz), the vibration of PCB can generate acoustic noise.

To evaluate the MLCC caused PCB vibration during early design stage, it is preferable to develop a proper simulation methodology for the PCB dynamic characteristics. Many research work have concentrated on the board fatigue failure prediction [7] and improvement of finite-element numerical methods [8]. The intrinsic board vibration properties are also investigated through modal analysis simulation [9], [10]. The forced PCB vibration subjected to MLCC vibration can also be analyzed through simulation with harmonic analysis [11]. However, the influence of MLCC location on the vibration amplitude is not considered and validated. In addition, the effect of board parameters to board vibration properties has not been clearly evaluated. Furthermore, there has been no demonstration to accommodate parameter variations in the modal analysis simulation.

This article is an extension for [12]. Compared to [12], the parameter effect is first analyzed from vibration theory. A statistical simulation method is also proposed to take the parameter variation effect into consideration. The simulated results are validated through the comparison with measurement. The effect of MLCC location on PCB vibration is also simulated and validated through measurement.

In this article, MLCC induced acoustic noise in mobile systems is studied through PCB vibration simulation investigation. The governing equations are summarized and analyzed to identify the key parameters. The understanding for vibration behavior is also derived from the theoretical analysis. A statistical simulation methodology is proposed to accommodate the key parameter variations in modal analysis. The obtained

modal shape patterns and natural frequencies are compared with measurement and are analyzed statistically. Through simulation, the contribution of each parameter can also be identified, thus allowing engineers to filter out less useful parameters during design stage. The MLCC location influence on PCB vibration is investigated through harmonic analysis with modal superposition. The forced vibration is also validated through measurement. With the intrinsic PCB vibration properties, the MLCC induced vibration can be predicted. More importantly, a design guideline can be proposed based on the analysis of the modal shape pattern. By placing the MLCC at locations with smaller amplitude in the modal shape response, the excited modal amplitude can be reduced, thus reducing the acoustic noise. Traditionally, the MLCC placement is mainly a consideration for PDN electrical performance. The proposed method can be applied together with the common MLCC placement design guidelines to improve both the acoustic noise performance and electrical performance.

II. Acoustic Noise Analysis From PCB Vibration Study

A. PCB Acoustic Noise Generation Mechanism

MLCCs connected on the PDN are subjected to the electrical noise presented on the power rail. The switching noise on the power rail can excite the MLCCs to vibrate. As the MLCCs are soldered on the PCB, which is a rigid connection, the PCB will vibrate follow the pace of the MLCCs. If the electrical noise is in the audible frequency range, the PCB vibration will produce the acoustic noise. It has been validated and demonstrated in many works [5], [11], [12] that the acoustic noise can be analyzed from the vibration study of the PCB. In addition, the vibration simulation can be conducted more conveniently than the acoustic noise simulation. In this article, the simulation methodology is proposed from the PCB vibration point of view.

B. PCB Vibration Governing Equation and Parameters

Assuming the board can be treated as a thin rectangular plate in *x*–*y* plane, the out-of-plane displacement can be written as the following wave equation [13]

$$\frac{Eh^3}{12\left(1-v^2\right)}\left(\frac{\partial^4 w}{\partial x^4}+2\frac{\partial^4 w}{\partial x^2\partial y^2}+\frac{\partial^4 w}{\partial y^4}\right)+\gamma\frac{\partial^2 w}{\partial t^2}=q \quad (1)$$

where w is the out-of-plane displacement, E represents the Young's modulus, v is for the Poisson's ratio, h is the plate thickness, t is the time, γ is the mass per unit area of the plate, and q is the out-of-plane pressure load (external force) in $+z$ direction.

If there is no external load forced on the structure, the intrinsic vibration properties of the board can be derived by solving (1), setting $q = 0$. The evaluation of the board intrinsic modes is referred as modal analysis. Applying separation of variables as $w(x,y,t) = \phi(x,y)T(t)$, (1) can be decoupled to an equation of space, x and y only

$$\frac{d^4\phi(x,y)}{dx^4}+\frac{d^4\phi(x,y)}{2dx^2dy^2}+\frac{d^4\phi(x,y)}{dy^4}-\omega^2\frac{12\left(1-v^2\right)\gamma}{Eh^3}\phi(x,y)=0 \quad (2)$$

which is a spatial eigenvalue equation. An equation of time only

$$\frac{d^2T(t)}{dt^2}+\omega^2T(t)=0 \quad (3)$$

$\phi(x, y)$ is the spatial mode shape, $T(t)$ is a function of time and ω is the circular natural frequencies.

To illustrate the properties of modal response, an example case where the four edges of the plates are fixed is examined. In real case, the fixation boundary conditions maybe more complicated. The modal solution from (2) for the simply supported rectangular plate with length a and width b can be expressed as

$$\phi_{ij}(x,y)=\sin\left(\frac{i\pi x}{a}\right)\sin\left(\frac{i\pi y}{b}\right), \quad i=1,2,3,\ldots,j=1,2,3,\ldots \quad (4)$$

where i and j are modal indices denoting the number of half waves in the mode shape along the x and y coordinates, respectively. The associated natural frequency $f_{ij} = \omega_{ij}/2\pi$ is

$$f_{ij}=\frac{1}{2\pi}\left[\left(\frac{i\pi}{a}\right)^2+\left(\frac{j\pi}{b}\right)^2\right]\sqrt{\frac{Eh^3}{12\gamma\left(1-v^2\right)}}. \quad (5)$$

The vibration modal response is in analogous to electromagnetic waves for a rectangular cavity.

If an external force is applied, the study of vibration characteristics with external force is referred as harmonic analysis. In this article, the forced dynamic response is obtained through modal superposition, which means that the displacement can be written as a linear combination of the Eigen modes

$$w(x,y,t)=\sum_i\sum_j\alpha_{ij}(t)\phi_{ij}(x,y) \quad (6)$$

where $\alpha_{ij}(t)$ is the *i*–*j*th modal amplitude under external force $F_0\cos(2\pi ft)$. $\phi_{ij}(x,y)$ is previously solved spatial mode shape for the *i*–*j*th mode. The modal amplitude is expressed as

$$\alpha_{ij}(t)=\frac{4F_0}{\gamma ab\omega_{ij}^2}\frac{\sin(i\pi x_0/a)\sin(j\pi y_0/b)}{1-f^2/f_{ij}^2}\cos(2\pi ft) \quad (7)$$

for the previously simply supported rectangular plate case. The external force is applied at (x_0, y_0) location.

From (7), it can be shown that the out-of-plane displacement will oscillate follow the frequency of the external force. Also, if the external force frequency is very close to the natural frequency, the modal amplitude will be very large, which will lead to board resonance. In addition, since the modal amplitude includes the $\sin(i\pi x_0/a)\sin(j\pi y_0/b)$ term which is of the same form as modal shape response $\sin(i\pi x/a)\sin(j\pi y/b)$, the location where the external force is applied is important.

This is also valid for other board boundary conditions [13]. If the force is applied at the location where the displacement is small for a particular mode response, the modal amplitude will also be small. On the contrary, if the force is imposed to the position where the displacement is large for a particular mode response, the modal amplitude will also be large.

TABLE I
BOARD STACK UP FROM VENDOR

Layer	Material	Thcikness Range (mil)
1	copper, 1/3oz	1.000~1.400
2	dielectric, 1037MR	1.573~1.973
3	copper, 1/3oz	0.650~0.950
4	dielectric, 1037HR	1.947~2.347
5	copper, 1/3oz	0.650~0.950
6	dielectric, 1037MR	1.577~1.977
7	copper, 1/2oz	0.500~0.800
8	dielectric, 1080 core	2.200~2.800
9	copper, 1/2oz	0.500~0.800
10	dielectric, 1080*2	4.835~6.035
11	copper, 1/2oz	0.500~0.800
12	dielectric, 1080 core	2.200~2.800
13	copper, 1/2oz	0.500~0.800
14	dielectric, 1037MR	1.573~1.983
15	copper, 1/3oz	0.650~0.950
16	dielectric, 1037HR	1.956~2.356
17	copper, 1/3oz	0.650~0.950
18	dielectric, 1037MR	1.646~2.046
19	copper, 1/3oz	1.000~1.400

III. STATISTICAL SIMULATION METHOD FOR PCB VIBRATION PROPERTIES

The PCB intrinsic vibration properties are firstly analyzed through modal analysis. From (4), it can be observed that the thin board modal shape is a function of board x–y direction geometry. From (5), it can be shown that the natural frequency is a function of board material properties, which include material mass density, Young's modulus and Poisson's ratio. It is also a function of board dimensions, including board x–y direction geometry and the board thickness. It can be shown that, for a specific boundary fixation condition, as long as the geometry in x–y direction can be correctly obtained, the mode shape can be solved rather easily. On the other hand, the natural frequency is more sensitive to the board thickness and material properties, as these parameters can vary up to about $\pm 20\%$ [14]. To address the influence of these parameter variations, a statistical simulation method is proposed.

A. Statistical Simulation Method

To build the device under test (DUT) PCB model for vibration simulation, each of the 19 layers of the DUT needs to be set properly. The layer thickness and dielectric material information are given in Table I, based on the stack-up specification provided by the PCB vendor.

For the statistical simulation model, three important parameters, the layer thickness, layer mass density, and layer Young's modulus, are swept in the given range to produce the distributed output results. These input parameters are subjected to relatively significant variation during the real fabrication process. The outputs of the statistical simulation model are the natural frequencies and the corresponding modal shapes. The process of the statistical simulation method is illustrated in Fig. 1.

Based on the PCB stack up information, the PCB vibration model for the nominal input parameters is first built. The initial model is constructed using Sherlock [15]. The materials for dielectric layers are selected from the material library. To account for the trace routing of different copper metal layers, the metal

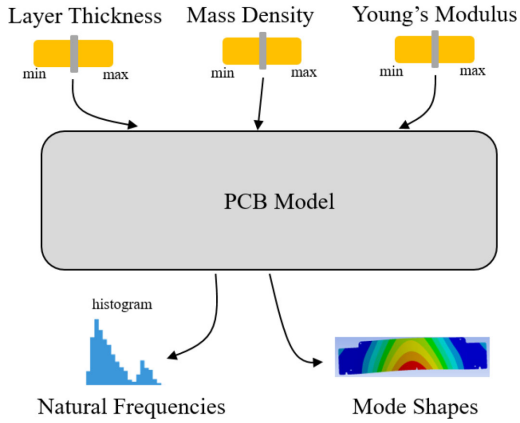

Fig. 1. Process of statistical simulation methodology.

L...	Material	Thickne...	Density	CTExy	CTEz	Exy	Ez
1	COPPER (68.3%) / COPPER-RESIN	1.28 mil	6.6493	27.871	27.871	78,288	78,288
2	EM-370Z / Resin Content (73.0%)	1.8 mil	1.7177	18.905	46.506	17,058	8,199
3	COPPER (68.1%) / COPPER-RESIN	0.85 mil	6.6351	27.936	27.936	78,070	78,070
4	EM-370Z / Resin Content (75.0%)	2.3 mil	1.7018	19.894	47.269	16,218	8,067
5	COPPER (93.0%) / COPPER-RESIN	0.85 mil	8.4030	19.868	19.868	105,335	105,335
6	EM-370Z / Resin Content (73.0%)	1.8 mil	1.7177	18.905	46.506	17,058	8,199
7	COPPER (56.8%) / COPPER-RESIN	0.68 mil	5.8328	31.597	31.597	65,696	65,696
8	EM-370Z / Resin Content (55.0%)	2.5 mil	1.8604	13.040	39.639	24,624	9,612
9	COPPER (95.0%) / COPPER-RESIN	0.69 mil	8.5450	19.220	19.220	107,525	107,525
10	EM-370Z / Resin Content (58.0%)	5.5 mil	1.8366	13.754	40.783	23,363	9,344
11	COPPER (94.8%) / COPPER-RESIN	0.65 mil	8.5308	19.285	19.285	107,306	107,306
12	EM-370Z / Resin Content (57.0%)	2.6 mil	1.8445	13.507	40.402	23,783	9,432
13	COPPER (57.9%) / COPPER-RESIN	0.69 mil	5.9109	31.240	31.240	66,900	66,900
14	EM-370Z / Resin Content (73.0%)	1.8 mil	1.7177	18.905	46.506	17,058	8,199
15	COPPER (94.5%) / COPPER-RESIN	0.7 mil	8.5095	19.382	19.382	106,978	106,978
16	EM-370Z / Resin Content (75.0%)	2 mil	1.7018	19.894	47.269	16,218	8,067
17	COPPER (82.7%) / COPPER-RESIN	0.81 mil	7.6717	23.205	23.205	94,057	94,057
18	EM-370Z / Resin Content (73.0%)	1.8 mil	1.7177	18.905	46.506	17,058	8,199
19	COPPER (90.3%) / COPPER-RESIN	1.24 mil	8.2113	20.743	20.743	102,378	102,378

Fig. 2. Stack up of board model for PCB vibration simulaiton.

layer is treated as a mixture of the copper and dielectric material calculated from board layout file. The aggregate mechanical properties of the 19 layers can then be derived automatically based on the layer material information.

The board vibration model stack up setting is depicted in Fig. 2. The copper layer is considered as copper-resin mixture, with the copper ratio indicated. For the power or ground layer where most of the layer area is covered with copper, the ratio will be close to 100%. The percentage of resin content for the dielectric material is determined by the laminate type. The difference of prepreg and core is also accounted for. Layer thickness is set to the nominal thickness indicated by the vendor. The mass density, coefficient of thermal expansion (CTExy, CTEz for in-plane, and out-of-plane) and modulus (Exy, Ez for in-plane, and out-of-plane) are calculated from the layer setting. For vibration simulation, the thickness, density and modulus are the critical parameters. The unit for density, CTE and modulus are g/cm^3, 10^{-6}/°C, and MPa, respectively.

The constructed initial board model is then imported to Ansys workbench [16] for statistical analysis. The initial board vibration model is plotted in Fig. 3. The board is fixed at the circled four locations. Other components on the board are ignored for simplicity. The value range for the board layer density and modulus are set to deviate from the initial nominal value with $\pm 20\%$. The design cases are generated with optisLang plugin

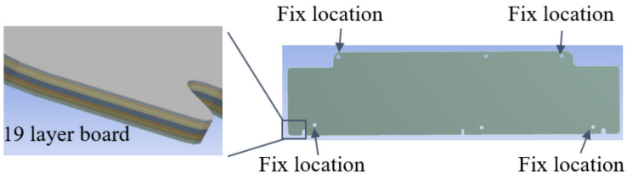

Fig. 3. PCB vibration model for modal analysis in Ansys workbench.

TABLE II
SIMULATED MODAL SHAPE RESULTS

Mode No.	1	2
Mode Pattern		
Mode No.	3	4
Mode Pattern	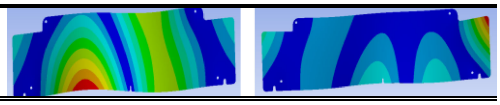	
Mode No.	5	6
Mode Pattern	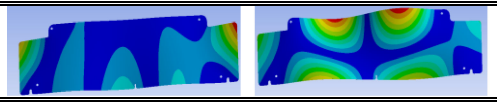	
Mode No.	7	8
Mode Pattern	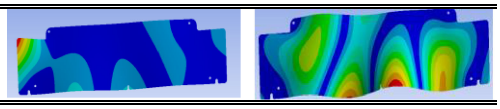	
Mode No.	9	10
Mode Pattern	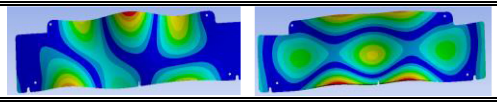	

[17] in the Ansys workbench, given the designated parameter scope. Three board layer thickness situations are evaluated to reduce simulation complexity, where each layer is set to the minimum value, nominal value and the maximum value, respectively. Under each board layer thickness condition, the board layer density, and modulus are varied and the corresponding mode shapes and frequencies are obtained. For each board layer thickness situation, 100 cases are generated. There are total of three hundred cases. For each thick thickness condition, the distribution is close to a Gaussian distribution. The histogram plot in Fig. 4 is a combination of the distribution of all the three layer thickness cases. The combined histogram looks like three "bundles" of Gaussian distribution. The left, middle, and right bundles correspond to the minimal, nominal and maximum thickness conditions. The design of experiments process is applied to allow efficient statistical sampling of the parameter space. As mentioned earlier, the mode shapes are mainly determined by the board dimension in the x–y direction, the mode shapes obtained for these design cases will be very similar. The simulated first ten mode shapes are given in Table II. On the contrary, since the natural frequencies are tightly correlated with layer thickness, mass density, and modulus, the three hundred

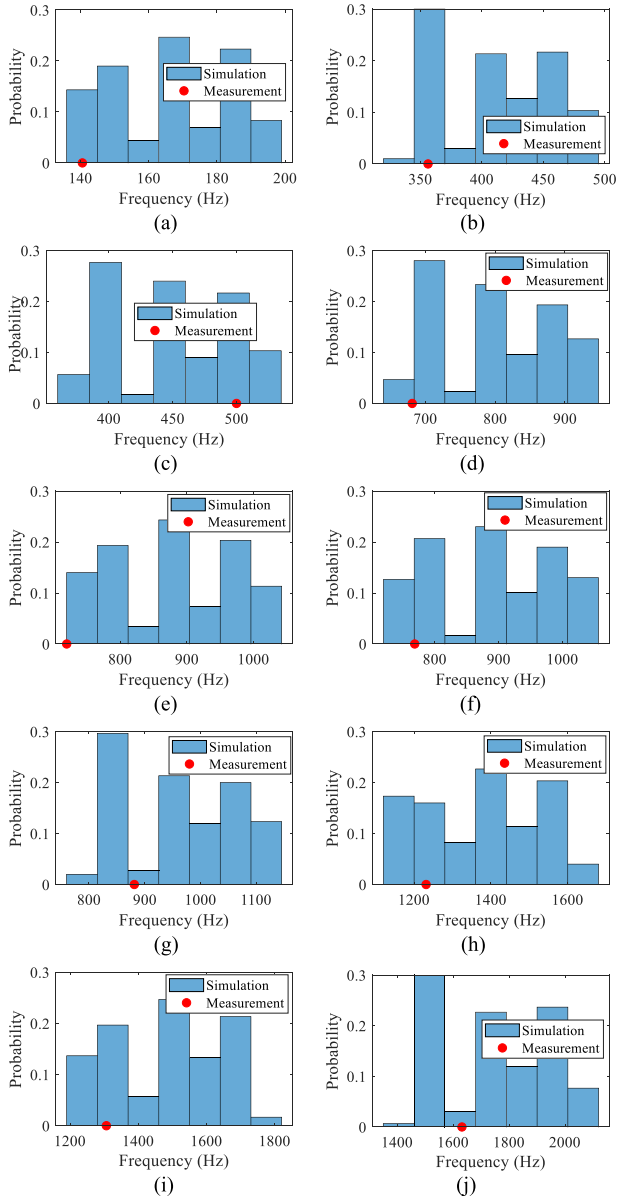

Fig. 4. Statistical distribution of natural frequency values for the first ten modes. (a) Mode 1. (b) Mode 2. (c) Mode 3. (d) Mode 4. (e) Mode 5. (f) Mode 6. (g) Mode 7. (h) Mode 8. (i) Mode 9. (j) Mode 10.

design cases will produce diverse mode frequency values. For the first ten modes, the probability distribution histograms of the natural frequency values are shown in Fig. 4.

B. Correlation With Measurement

The simulated mode shapes and natural frequencies are validated through measurement. The measurement setup is shown in Fig. 5. The bare board vibration is captured by a laser Dopper vibrometer [18]. The board is excited by applying an electrical signal on a capacitor hooked to the PDN power rail. Only one capacitor is soldered on the power rail for the evaluation. The location of the capacitor is indicated in the attached plot in Fig. 6 with red dot. The electrical signal exhibits uniform amplitude in

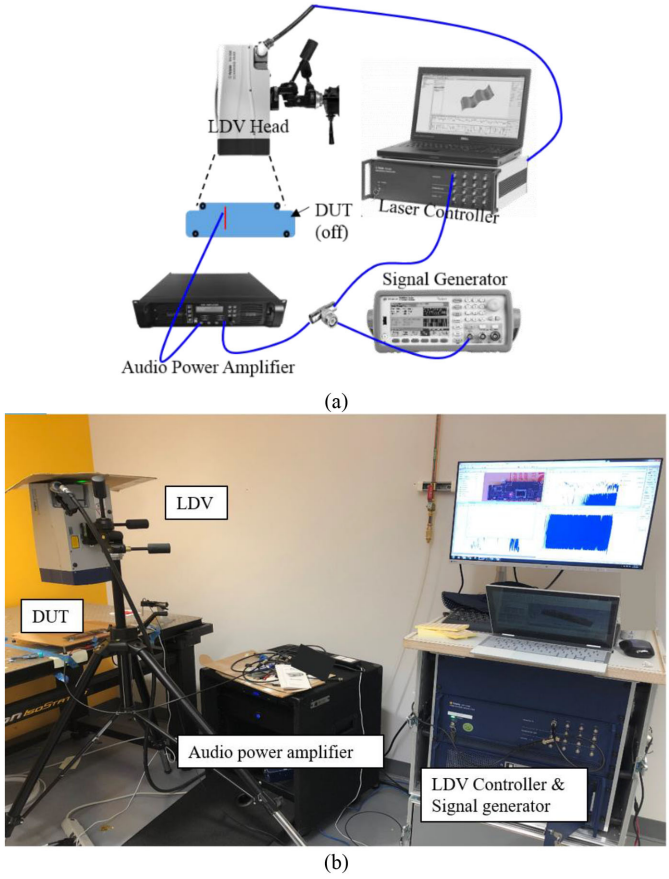

Fig. 5. Mode shapes measurement setup. (a) Setup illustration. (b) Scene photo of measurement.

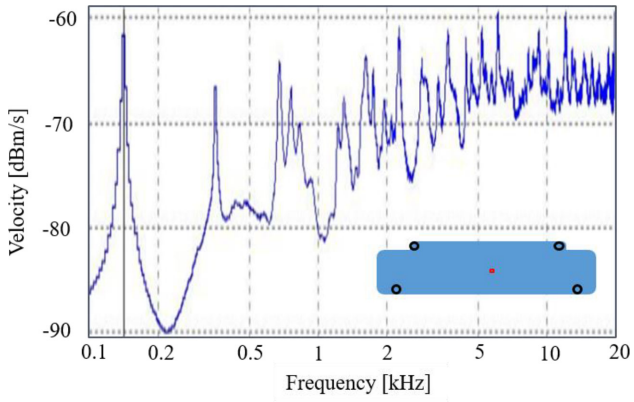

Fig. 6. Averaged vibration velocity spectrum for modal analysis.

the entire audio frequency range. The bare board is also fixed at the same four locations as in the simulation.

The board vibration is described with vibration velocity. The vibration spectrum at each scanning location is averaged to obtain an averaged vibration spectrum as illustrated in Fig. 6. The peak locations corresponds to the natural frequencies. The vibration "hot map" at these frequencies are the related mode shape patterns.

TABLE III
MEASURED MODAL RESULTS

Mode No.	1	2
Mode Pattern	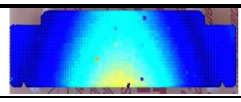	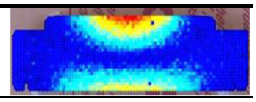
Natural Freq.	140.6Hz	356.3Hz
Mode No.	3	4
Mode Pattern	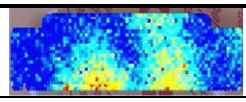	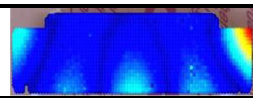
Natural Freq.	500Hz	681.3Hz
Mode No.	5	6
Mode Pattern	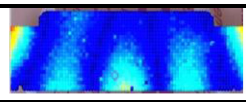	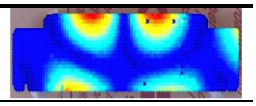
Natural Freq.	720Hz	800Hz
Mode No.	7	8
Mode Pattern	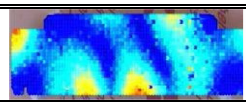	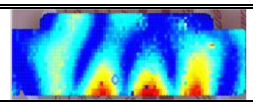
Natural Freq.	881.2Hz	1231.2Hz
Mode No.	9	10
Mode Pattern	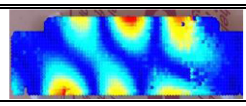	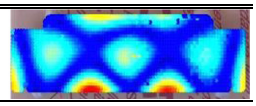
Natural Freq.	1306.3Hz	1631.3Hz

The measured first ten mode shapes are summarized in Table III. It can be shown that, with the proposed simulation procedure, the board modal shape patterns can be estimated rather close to the real measurements. In addition, for the simulated natural frequency histogram, the frequency values in the horizontal axis are the possible values that could exist for the corresponding mode based on the range of the given parameters. With the proposed statistical simulation method, engineers can evaluate the board intrinsic vibration properties with reasonable flexibility based on the board stack up information.

C. *Parameter Sensitivity Analysis*

The uncertainty in the output response of the board vibration system can be divided and allocated quantitatively to different sources of uncertainty in its input. The sensitivity analysis for mode frequencies with respect to the layer mass density and layer modulus is conducted to understand the dominant parameters controlling board vibration properties. These effects are evaluated at a fixed layer thickness. The sensitivity to layer thickness is not evaluated in this process. However, the effect of layer thickness can be observed in Fig. 4. For different layer thickness, the sensitivity results to each layer mass density and layer modulus are very similar. The effect of each layer density and modulus to the first ten natural frequencies is summarized in Fig. 7. Some parameters with contribution less than 0.4%

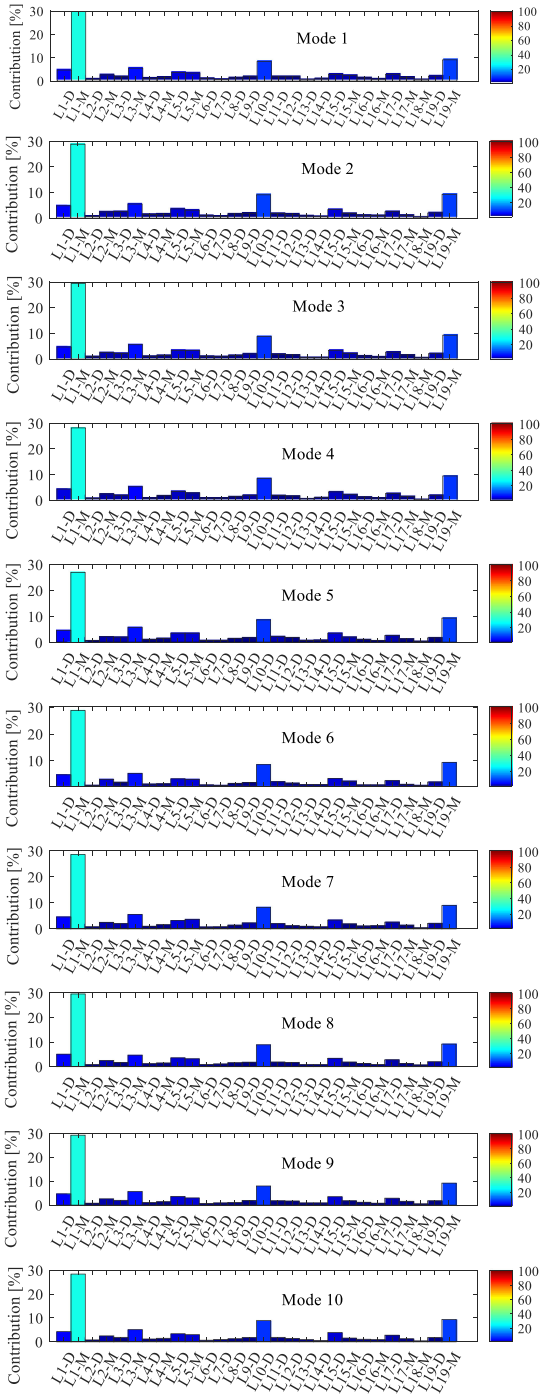

Fig. 7. Layer mass density (L*_D) and layer modulus (L*_M) influence percentage to the mode frequencies.

are not shown. The percentage of each colored bar indicates the corresponding input parameter influence on the corresponding output response. For a certain output response (one natural frequency), the total effect of all the parameters added together is very close to 1.

It can be observed that, for all the mode frequencies, the first layer modulus is the dominant factor. The secondary influential input parameter is the last layer modulus. The top and bottom layers are both copper-resin mixture. Since the top layer and the bottom layers are not bounded by the other layers on one side, the layer modulus effect will be stronger. In addition, the top layer possesses less copper percentage, this could be the reason that the top layer modulus is more dominant than that of the bottom layer. On the other hand, the mass density of the tenth layer also exhibit comparable influence as with the bottom layer modulus. This may be due to the fact that the tenth layer is the thickest layer among all the other layers. Based on the understanding of the dominant input parameters, the intrinsic board vibration properties can be predicted or evaluated with ease.

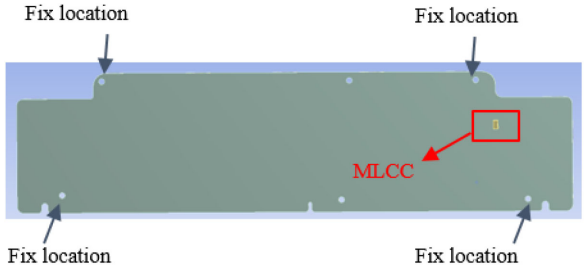

Fig. 8. PCB model for harmonic analysis in simulation.

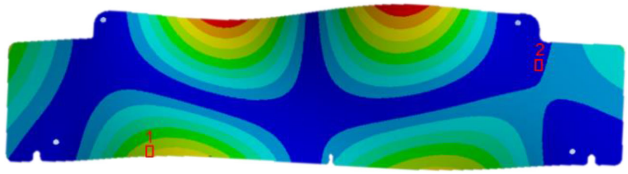

Fig. 9. MLCC excitation location respective to mode 6 response.

IV. PCB Vibration Due to MLCC Vibration Excitation

From the modal analysis, the intrinsic board vibration properties can be predicted. With the modal response, the board vibration under external forces can be calculated based on (10). As mentioned before, the board vibration subject to the external force is evaluated through harmonic analysis applying modal superposition. For the harmonic analysis, an MLCC is added to the top layer and an external force is applied to the top layer of the MLCC to mimic the situation where the MLCC is vibrating. The simulation model for the harmonic analysis is plotted in Fig. 8. The board is fixed at the same four locations.

As previously discussed for (10), the capacitor excitation location is critical to the resulted board vibration response. If the capacitor is placed at locations where the modal response is small, the forced vibration response will also be small. On the contrary, if the capacitor is placed at locations where the modal response is relatively high, the induced forced vibration response will be stronger. To examine the effect of MLCC excitation locations on vibration strength, two capacitor excitation locations are selected. The board vibration is evaluated at the mode 6 frequency. Since the size of the capacitor is relatively small, the change of the modal response is negligible. The checked capacitor locations with respect to the mode 6 response are depicted in Fig. 9. The forced vibration simulation results are illustrated in Fig. 10(a) and (b). The first capacitor location is

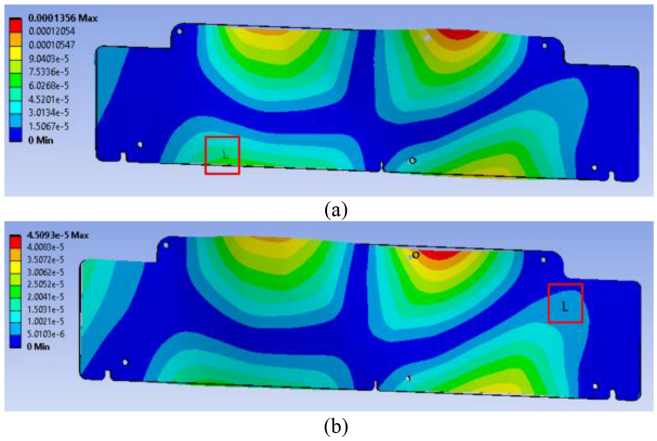

Fig. 10. Simulated PCB vibration with MLCC excitation at different locations. (a) Location 1. (b) Location 2.

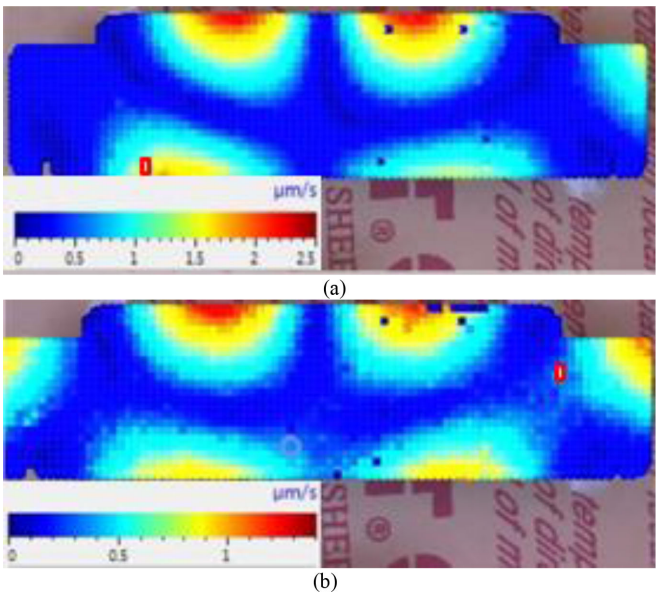

Fig. 11. Measured PCB vibration with MLCC excitation at different locations. (a) Location 1. (b) Location 2.

selected at the position where the mode 6 mode response is relatively strong, while the second capacitor location is selected at the position where the mode 6 mode response is relatively weak. For the two cases, the amplitude of excitation force applied to the top surface of the capacitor are kept to the same as 0.5 N. The highest vibration amplitude induced for location 1 is 1.356e-4 m, while the generated highest vibration amplitude for location 2 is 4.5e-5 m.

The effect of the capacitor excitation location is also validated on the real board measurement. The measurement setup is the same as shown in Fig. 5. The board is excited by applying a broad band signal to the MLCC and the mode 6 is examined. The excitation voltages are kept to the same for the two cases. The capacitor locations in the two cases are exactly the same as in the simulation setup. The vibration response for the two capacitor locations is depicted in Fig. 11. From the reading of the averaged vibration spectrum at the mode 6 frequency as

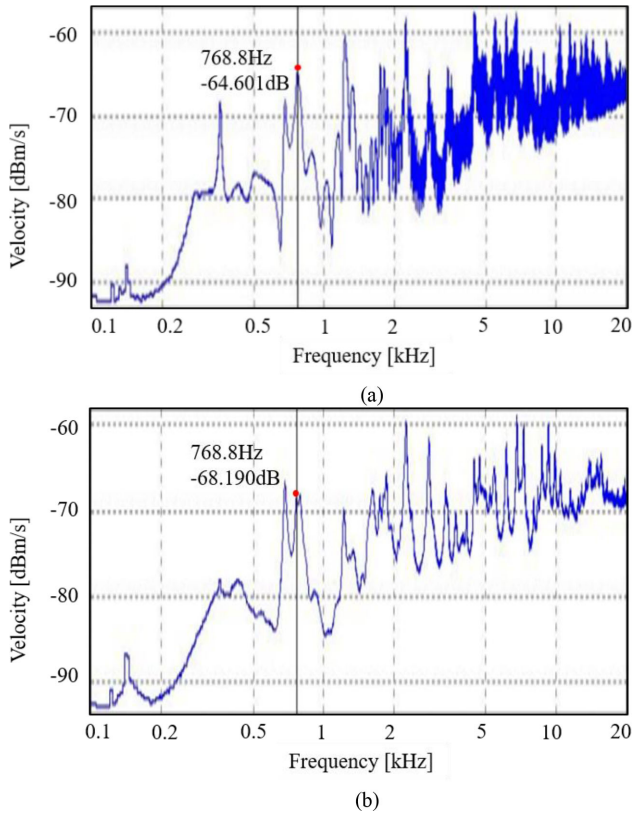

Fig. 12. Measured PCB vibration spectrum with MLCC excitation at different locations. (a) Location 1. (b) Location 2.

shown in Fig. 12, the averaged vibration velocity for location 1 is −64.6014 dBm/s, while for location 2 is −68.190 dBm/s.

The evaluation of the intrinsic board vibration properties is important, as it can provide design guidelines for placing the capacitors and avoiding the resonance frequencies. In real practice, eliminating the power rail noise in the audio frequency range maybe difficult. However, with the mode shape response, it is possible to identify several area where the mode shape response is weak and put the decoupling capacitor for the power rail at these identified locations. In addition, the forced vibration analysis can also be conducted based on the modal analysis.

V. Conclusion

In this article, a statistical simulation methodology for PCB intrinsic vibration properties is proposed to include the effect of parameter variation. The key parameters are identified through the analysis of PCB vibration governing equations. The variation range information can be gathered from PCB vendor. The studied parameters are board layer thickness, mass density, and Young's modulus. Since the modal shape response is mainly a function of the in plane dimension of the board, the acquired mode shape patterns are very similar in all the design cases. The simulated mode shape patterns are very close to the measurement results. The natural frequencies are controlled by all the aforementioned parameters, thus a statistically distributed result can be obtained. The measured natural frequencies can fall into the range of the simulated distribution scope, indicating

the capability of the proposed statistical simulation model. The MLCC induced PCB vibration is simulated through harmonic analysis applying modal superposition method. Based on the intrinsic PCB vibration response, a design guideline is proposed regarding the MLCC placement. Putting MLCCs at the "blue" regions in modal shape response, the excited related modal amplitude will be smaller, thus reducing the level of vibration. This conclusion is draw first from the previous theoretical study and then validated with harmonic simulation. The simulated results for MLCC induced PCB vibration is also validated through measurement.

REFERENCES

[1] L. D. Smith, R. E. Anderson, D. W. Forehan, T. J. Pelc, and T. Roy, "Power distribution system design methodology and capacitor selection for modern CMOS technology," *IEEE Trans. Adv. Packag.*, vol. 22, no. 3, pp. 284–291, Aug. 1999.

[2] C. Hwang, J. Kim, B. Achkir, and J. Fan.. "Analytical transfer functions relating power and ground voltage fluctuations to jitter at a single-ended full-swing buffer," *IEEE Trans. Compon., Packag. Manuf. Technol.*, vol. 3, no. 1, pp. 113–125, Jan. 2013.

[3] S. Das, P. Whatmough, and D. Bull, "Modeling and characterization of the system-level power delivery network for adual-core ARM Cortex-A57 cluster in 28nm CMOS," in *Proc. IEEE Int. Symp. Low Power Electron. Des.*, Jul. 2015, pp. 146–151.

[4] Y. Sun, J. Kim, and C. Hwang, "Jitter-aware target impedance," in *Proc. IEEE Int. Symp. Electromagn. Compat.*, Jul. 2019, pp. 217–222.

[5] B. H. Ko, S. G. Jeong, Y. G. Ahn, K. S. Park, N. C. Park, and Y. P. Park, "Analysis of the correlation between acoustic noise and vibration generated by a multi-layer ceramic capacitor," *Microsyst. Technol.*, vol. 20, no. 8-9, pp. 1671–1677, Aug. 2014.

[6] T. L Jordan, and Z. Ounaies, "Piezoelectric ceramics characterization." Nat. Aeronaut. Space Admin. Washington, DC, USA, ICASE Rep. 2001-28, Sep. 2001.

[7] Q. J. Yang, H. L. J. Pang, Z. P. Wang, G. H. Lim, F. F. Yap, and R. M. Lin, "Vibration reliability characterization of PBGA assemblies," *Microelectron. Rel.*, vol. 40, no. 7, pp. 1097–1107, Jul. 2000.

[8] S. Rzepka, F. Kramer, O. Grassmé, and J. Lienig, "A multilayer PCB material modeling approach based on laminate theory," in *Proc. Therm. Mech. Multi-Phys. Simul. Exp. Microelectron. Micro-Syst.*, Apr. 2008, pp. 1–10.

[9] S. Park *et al.*, "Transient dynamic simulation and full-field test validation for a slim-PCB of mobile phone under drop/impact," in *Proc. Elect. Compon. Technol. Conf.*, May 2007, pp. 914–923.

[10] Y. Wang, K. H. Low, H. L. J. Pang, K. H. Hoon, F. X. Che, and Y. S. Yong, "Modeling and simulation for a drop-impact analysis of multi-layered printed circuit boards," *Microelectron. Rel.* vol. 46, no. 2-4, pp. 558–573, Feb. 2006.

[11] H. Kim, D. Kim, N. C. Park, and Y. P. Park, "Acoustic noise and vibration analysis of solid state drive induced by multi-layer ceramic capacitors," *Microelectron. Rel.*, vol. 83, pp. 136–145, Apr. 2018.

[12] Y. Sun, J. Zhang, Z. Yang, C. Hwang, and S. Wu, "Simulation investigation on acoustic noise caused by 'singing' capacitors on mobile devices," in *Proc. IEEE Int. Symp. Electromagn. Compat.*, Jul. 2019, pp. 406–410.

[13] R. D. Blevins, *Formulas for Dynamics, Acoustics and Vibration*. New York, NY, USA: Wiley, 2015.

[14] S. Sakata, K. Okuda, and K. Ikeda, "Stochastic analysis of laminated composite plate considering stochastic," *Frontiers Struct. Civil Eng.*, vol. 9, no. 2, pp. 141–153, Jun. 2015.

[15] Sherlock, Ansys, Canonsburg, PA, USA, 2019. [Online]. Available: https://www.ansys.com/products/structures/ansys-sherlock

[16] Ansys workbench, Ansys, Canonsburg, PA, USA, 2019. [Online]. Available: https://www.ansys.com/products/structures

[17] optiSLang, Ansys, Canonsburg, PA, USA, 2019. [Online]. Available: https://www.ansys.com/products/platform/ansys-optislang

[18] Y. Sun, S. Wu, Z. Yang, C. Hwang, and J. Zhang, "Measurement methodologies for acoustic noise induce by multilayer ceramic capacitors of power distribution network in mobile systems," vol. 62, no. 4, pp. 1515–1523, Aug. 2020.

Yin Sun (Student Member, IEEE) received the B.S. degree in microelectronics from Fudan University, Shanghai, China, in 2013, and the M.S. degree in electrical and computer engineering from the Hong Kong University of Science and Technology, Hong Kong, in 2016. She is currently working toward the Ph.D. degree in electrical engineering at the Electromagnetic Compatibility Laboratory, Missouri University of Science and Technology (formerly University of Missouri-Rolla), Rolla, MO, USA.

Her current research interests include radio frequency interference in mobile devices, EMI source modeling and prediction, power supply induced jitter in I/O buffer, power distribution network target impedance design, signal/power integrity in high-speed digital systems, and acoustic noise in multilayer ceramic capacitors.

Songping Wu (Senior Member, IEEE) received the B.S. degree from Wuhan University, Wuhan, China, in 2003, the M.S. degree from the Huazhong University of Science and Technology, Wuhan, China, in 2006, and the Ph.D. degree in electrical engineering from the Missouri University of Science and Technology, Rolla, MO, USA, in 2011.

From 2011 to 2012, he was a Hardware Engineer with Cisco Systems, San Jose, CA, USA. From 2012 to 2016, he was a Senior Signal Integrity engineer with Apple, Cupertino, CA, USA. He is currently a desense/SI Engineer with Google Consumer Hardware Group, Mountain View, CA, USA. Since 2016, he has been with SIPI lead of Chromebook with Google Inc., Mountain View, CA, USA. His current research interest includes in-device desense and co-existence in consumer hardware systems as well as signal integrity and power integrity issues in package and high-speed printed circuit boards (PCBs) for digital devices and systems, and application of signal integrity in sensors.

Dr. Wu was the recipient of the IEEE Electromagnetic Compatibility.

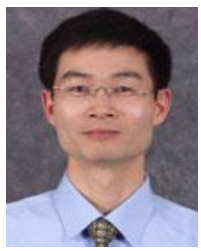

Jianmin Zhang (Senior Member, IEEE) received the M.S. and Ph.D. degrees in electrical engineering from EMC Laboratory, University of Missouri-Rolla, Rolla, MO, USA, in 2003 and 2007, respectively.

He is currently a Hardware Engineer with Google, Menlo Park, CA, USA. Before joining Google, he was a Principal SI/PI Engineer with Apple, a SMTS Engineer with Altera Corporation and a Technical Leader with Cisco Systems. He has published more than 50 technical papers and reviewed more than 200 academic papers for journals, international conferences and book proposals. He has served as technical committee members, review board members, session chairs and co-chairs for IEEE EMC Society, DesignCon, and EMC Europe. His current research interests include signal and power integrity for both network systems and mobile systems, RF desense and co-existence modeling and analysis, and acoustic noise modeling and analysis.

Dr. Zhang was the recipient of the Technical Achievement Award from IEEE EMC Society in 2019 for contributions to the understanding and practice of RF de-sense and co-existence through modeling and measurements, and application in product design. He was the Co-Advisor of the Best Student Symposium Paper Award from IEEE EMC Society for year 2018 and 2010. He was also recipient of the Conference Best SI Paper Award from the International Microelectronics and Packaging Society in 2007, and the Best Symposium Paper Award and the Best Student Symposium Paper Award from IEEE EMC Society in 2006.

Chulsoon Hwang (Senior Member, IEEE) received the B.S., M.S., and Ph.D. degrees in electrical engineering from the Korea Advanced Institute of Science and Technology, Daejeon, South Korea, in 2007, 2009, and 2012, respectively.

From 2012 to 2015, he was a Senior Engineer with the Global Technology Center, Samsung Electronics, Suwon, South Korea, where he was mainly engaged in radio-frequency interference design for mobile phones. In July 2015, he was with the Missouri University of Science and Technology (formerly University of Missouri-Rolla), Rolla, MO, USA, and is currently an Assistant Professor with the Missouri S&T EMC Laboratory. His current research interests include signal/power integrity in high-speed digital systems, inter/intra system EMI, hardware security and machine learning.

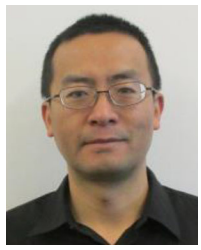

Zhiping Yang (Senior Member, IEEE) received the B.S. and M.S. degrees from Tsinghua University, Beijing, China, in 1994 and 1997, respectively, and the Ph.D. degree from the University of Missouri-Rolla, Rolla, MO, USA, in 2000, all in electrical engineering.

From 2000 to 2005, he was a Technical Leader with Cisco Systems, San Jose, CA, USA. From 2005 to 2006, he was a Principal Engineer with Apple Computer, Cupertino, CA, USA. From 2006 to 2012, he worked in Nuova Systems (which was acquired by Cisco in 2008) and Cisco Systems, San Jose, CA, as a Principal Engineer. From 2012 to 2015, he was a Senior Manager with Apple, Cupertino, CA, USA. He is currently a Senior Hardware Manager with Google Consumer Hardware Group, Mountain View, CA, USA. He has authored or coauthored more than 40 research papers and 17 patents. His research and patents have been applied in Google Chromebook, Apple iPhone 5S/6/6S, Cisco UCS, Cisco Nexus 6K/4K/3K, and Cisco Cat6K products. His current research interests include signal integrity and power integrity methodology development for Die/Package/Board co-design, high-speed optical module, various high-speed cabling solutions, high-speed DRAM/storage technology, high-speed serial signaling technology, and RF interference.

Dr. Yang was the recipient of the 2016 IEEE EMCS Technical Achievement Award.